Mitochondrial dysfunction and HIF1α stabilization in inflammation

Assegid Garedew and Salvador Moncada

Journal of Cell Science 125, 3254

doi: 10.1242/jcs.115949

Retraction of: *J. Cell Sci*. **121**, 3468-3475.

The authors wish to retract the above paper. We have recently identified errors affecting certain figure panels in Fig. 5 in which control data were processed inappropriately such that the figure panels do not accurately report the original data. The misuse and re-use of western blot bands violates the editorial policy of *Journal of Cell Science*, and so we must retract this article. A. G. regrets the inappropriate figure manipulations, of which his co-author was completely unaware.

We sincerely apologize to the scientific community for any confusion or adverse consequences resulting from the publication of these data.

Mitochondrial dysfunction and HIF1α stabilization in inflammation

Assegid Garedew and Salvador Moncada*

The Wolfson Institute for Biomedical Research, University College London, Gower Street, London WC1E 6BT, UK

*Author for correspondence (e-mail: s.moncada@ucl.ac.uk)

Accepted 8 July 2008
J. Cell Sci. 121, 3468-3475 Published by The Company of Biologists 2008
doi:10.1242/jcs.034660

Summary

Activation of murine-derived J774.A1 macrophages with interferon γ and lipopolysaccharide leads to a progressive mitochondrial defect characterized by inhibition of oxygen consumption and a decrease in the generation of ATP by oxidative phosphorylation. These changes are dependent on the generation of nitric oxide (NO) by an inducible NO synthase that becomes a significant consumer of oxygen. Furthermore, in these activated cells there is a biphasic stabilization of the hypoxia-inducible factor HIF1α, the second phase of which is also dependent on the presence of NO. The mitochondrial defect and stabilization of HIF1α synergize to activate glycolysis, which, at its maximum, generates quantities of ATP greater than those produced by non-activated cells. Nevertheless, the amount of ATP generated is not sufficient to fulfil the energy requirements of the activated cells, probably leading to a progressive energy deficit with the consequent inhibition of cell proliferation and death.

Key words: Nitric oxide, Mitochondria, HIF1α, Inflammation, Glycolysis, Oxidative phosphorylation

Introduction

It has been known for some years that nitric oxide (NO) decreases O_2 consumption in cells by inhibiting cytochrome c oxidase (Cox, complex IV) reversibly and in competition with O_2 (Cleeter et al., 1994; Brown and Cooper, 1994; Schweizer and Richter, 1994). In addition, prolonged exposure to NO leads to non-competitive and persistent inhibition of complex I and other key respiratory enzymes by S-nitrosylation (Clementi et al., 1998; Orsi et al., 2000a; Beltran et al., 2000a); such persistent inhibition can be enhanced by hypoxia (Frost et al., 2005). These findings prompted us to suggest that tissue dysoxia, which is characteristic of septic shock, is due to overproduction of NO, resulting in mitochondrial defect with the consequent decrease in the extraction of O_2 by tissues, leading ultimately to multiple organ failure and death (Rees et al., 1998; Orsi et al., 2000b). In recent years, evidence in favour of this hypothesis has been accumulating, including the demonstration of a significant mitochondrial defect in biopsies of skeletal muscle of individuals with sepsis (Brealey et al., 2002), the observation of an NO-dependent defect in complex I of biopsies obtained from animals with septic shock (Protti et al., 2007) and the preservation of mitochondrial activity in a septic shock model in inducible nitric oxide synthase (iNOS) knockout mice (Esmes et al., 2007). NO, which is produced in large quantities by iNOS, is also known to be involved in localized acute and chronic inflammation and degenerative disorders, we suggest that a similar mitochondrial defect to that observed in septic shock is likely to occur in such conditions (Moncada and Erusalimsky, 2002). Accumulating evidence suggests that this indeed may be the case in diseases of the nervous system such as Parkinson's, Alzheimer's and Huntington's, and amyotrophic lateral sclerosis (for reviews, see Lin and Beal, 2006; Schapira, 2006; Whitton, 2007). Although it is likely that such a defect may occur in other conditions associated with inflammation, such as metabolic syndrome or diabetes mellitus, the evidence is at present contradictory (Mogensen et al., 2007; Boushel et al., 2007; Nicolson, 2007).

Hypoxia-inducible factor (HIF)-1 is normally activated by hypoxia as a result of stabilization of its α-subunit (Jiang et al., 1996). It has recently been shown, however, that bacterial infection and inflammation stabilize HIF1α in macrophages (MΦ) in a way that is independent of hypoxia (Peyssonnaux et al., 2005). Such activation is important for the bactericidal activities of neutrophils and MΦ (Cramer et al., 2003; Peyssonnaux et al., 2005). One of the major responses of tissues to both inhibition of mitochondrial activity and expression of HIF1 is an increase in glycolysis by a variety of mechanisms, including gene expression (Semenza et al., 1994; Ebert et al., 1995). Furthermore, it has recently been reported that HIF1 downregulates mitochondrial activity during hypoxia by upregulating pyruvate dehydrogenase kinase 1 (PDK1) (Papandreou et al., 2006; Kim et al., 2006).

Because of these observations we decided to investigate, in J774.A1 murine MΦ activated with interferon (IFN)γ and lipopolysaccharide (LPS), the time course of the NO-induced mitochondrial defect, the role of NO in HIF1α stabilization, and the interplay between NO and HIF1α in the upregulation of glycolytic metabolism. In addition, we studied the bioenergetic consequences of these changes in terms of cell survival and proliferation.

Results

The majority of the time course experiments and biochemical assays were carried out with samples collected within the first 12 hours after activation with IFNγ (10 U ml^{-1}) and LPS (10 ng ml^{-1}), at which time there was no significant difference in cell viability ($P>0.05$, ANOVA) between control and treatment groups (data not shown). However, where indicated, some experiments were continued for a 24-hour observation period.

Effect of MΦ activation on O_2 consumption

Cellular O_2 consumption is the sum of mitochondrial and non-mitochondrial consumption. In our experiments, non-activated J774.A1 MΦ consumed O_2 at a rate of 49.1±2.6 pmol O_2 $second^{-1}$

10^{-6} cells, of which 48.0±1.7 was mitochondrial (Fig. 1A). Of the mitochondrial O_2 consumption, 37.6±3.3 pmol O_2 $second^{-1}$ 10^{-6} cells was oligomycin-sensitive and therefore attributable to oxidative phosphorylation (OXPHOS) (Fig. 1A), whereas the remaining 10.4±1.1 pmol O_2 $second^{-1}$ 10^{-6} cells could be accounted for by the so-called proton leak (Brand et al., 2005; Yadava and Nicholls, 2007). These values remained unchanged in non-activated MΦ and also for the first 3 hours after activation. However, as activation progressed, the mitochondrial consumption of O_2 decreased progressively to 13.2±0.8 pmol O_2 $second^{-1}$ 10^{-6} cells (27.5% of the control) at 12 hours. The O_2 consumption due to oxidative phosphorylation was the most affected as it decreased to 4.8±1.5 pmol O_2 $second^{-1}$ 10^{-6} cells (12.8% of the control), while the O_2 used by the proton leak decreased only slightly, to 8.4±0.9 pmol O_2 $second^{-1}$ 10^{-6} cells (80.8% of the control; $P<0.05$, paired *t*-test). These mitochondrial defects were concomitant with the release of NO into the extracellular fluid, which was first detected 4 hours after activation, and were prevented when the NO synthase inhibitor S-ethyl isothiourea (SEITU, 500 µM) was co-administered with IFNγ and LPS at the start of the experiment (Fig. 1A).

Mitochondrial spare respiratory capacity is the ability of mitochondria to increase O_2 consumption when more energy is required; this occurs because under basal conditions the enzyme is not working at its maximum rate. Spare respiratory capacity is calculated as the difference between the mitochondrial O_2 consumption under basal conditions and the maximal mitochondrial O_2 consumption, determined by uncoupling the respirator[illegible]hain with an optimal concentration of carbonyl cyan[illegible] (trifluoromethoxy)phenylhydrazone (FCCP). Treatment o[illegible]non-activated MΦ with FCCP showed them to have a spare respira[illegible]ry capacity of 56.3±4.3 pmol O_2 $second^{-1}$ 10^{-6} cells (Fig. 1B), wh[illegible] represented an increase of 117% in the [illegible]ndrial O[illegible] consumption. In activated MΦ, the spare [illegible]espirator[illegible] capacity started to decline between 2 and 3 hours [illegible]er activati[illegible] and was completely abolished within 5 hours, at wh[illegible] time [illegible]ere was only 55% inhibition of the basal mitochond[illegible]l O_2 c[illegible]ption (see Fig. 1A,B). The decline in the spare [illegible]acity of ac[illegible]ted MΦ was completely abolished by SEITU [illegible] 1B).

Non-mitochondrial O_2 con[illegible]mpti[illegible]n non-activated MΦ was 1.1±0.5 pmol O_2 $second^{-1}$ 1[illegible] cells. T[illegible] began to increase at 4 hours after activation ([illegible]t shown) and [illegible]reafter increased progressively to 13.8±3[illegible] pmol O_2 $second^{-1}$ 10[illegible]lls after 12 hours (Fig. 1C). Treatme[illegible] with S[illegible]ITU at the time of activation significantly reduc[illegible] this to [illegible]±0.2 pmol O_2 $second^{-1}$ 10^{-6} cells (not shown). The i[illegible] mito[illegible]ondrial O[illegible]onsumption of activated MΦ was also reduced [illegible]9% with [illegible]ITU and by 45% with 10 µM of the [illegible]vengel [illegible]haem[illegible]globin (HbO_2), administered 12 hour[illegible] after [illegible]tivation ([illegible] 1C). Addition of a higher concen[illegible]ation of HbO_2 had no [illegible]urther effect. After 24 hours of acti[illegible]n, all th[illegible] by the cells was non-mitochondrial; nearly [illegible] o[illegible]his was due to the activity of iNOS, as it could be inhibited b[illegible]ITU (not shown).

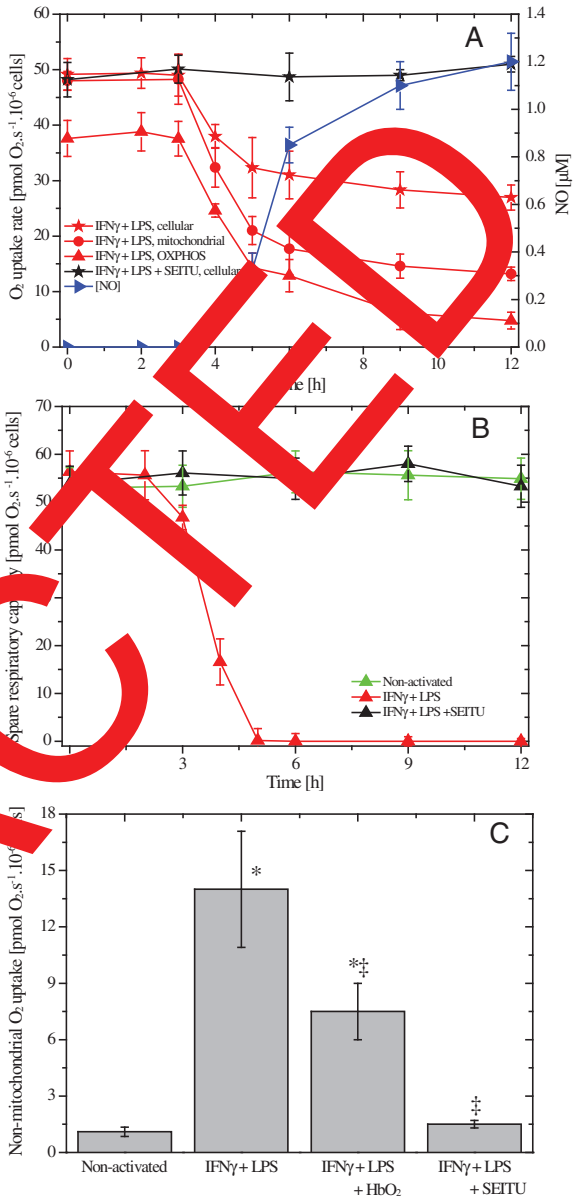

Fig. 1. Effect of activation of J774.A1 MΦ on their consumption of O_2 and generation of NO. Activation of MΦ with 10 U ml^{-1} IFNγ and 10 ng ml^{-1} LPS progressively inhibited mitochondrial O_2 consumption and concomitantly increased the release of NO into the extracellular fluid (A), and decreased the spare respiratory capacity (B). The different components of cellular O_2 consumption by untreated and SEITU-treated control MΦ did not change throughout the experimental period. Administration of 500 µM SEITU at the time of activation prevented the decrease in cellular (A) and mitochondrial O_2 consumption (not shown) and spare respiratory capacity (B). (C) The non-mitochondrial uptake of O_2 was greatly enhanced after 12 hours of activation; this could be reduced by the administration of 10 µM oxyhaemoglobin or abolished by treatment with SEITU. *, Significantly different from values in non-activated cells; ‡, Significantly different from IFNγ+LPS-treated cells ($P<0.05$, one way ANOVA, Tukey's post hoc test). Results are mean±s.d., $n=5$.

Effect of MΦ activ[illegible]on on glycolytic metabolism

Non-activated MΦ consumed glucose at a rate of 0.5±0.09 µmol $hour^{-1}$ 10^{-6} cells and released lactate at a rate of 0.6±0.05 µmol $hour^{-1}$ 10^{-6} cells. The activity of the glycolytic marker enzyme lactate dehydrogenase (LDH) in these cells was 0.96±0.04 IU 10^{-6} cells. None of these parameters changed significantly in untreated cells or in cells treated with only SEITU for up to 12 hours (Fig. 2A-C). Activation led to an increase in glycolytic metabolism that was evident even at 3 hours, before the inhibition of mitochondrial respiration. The rate of glucose consumption increased to 1.3±0.2 µmol $hour^{-1}$ 10^{-6} cells at 12 hours (Fig. 2A). The rate of lactate release followed a similar pattern, increasing to 2.3 µmol $hour^{-1}$ 10^{-6} cells at 12 hours (Fig. 2B). LDH activity also increased after

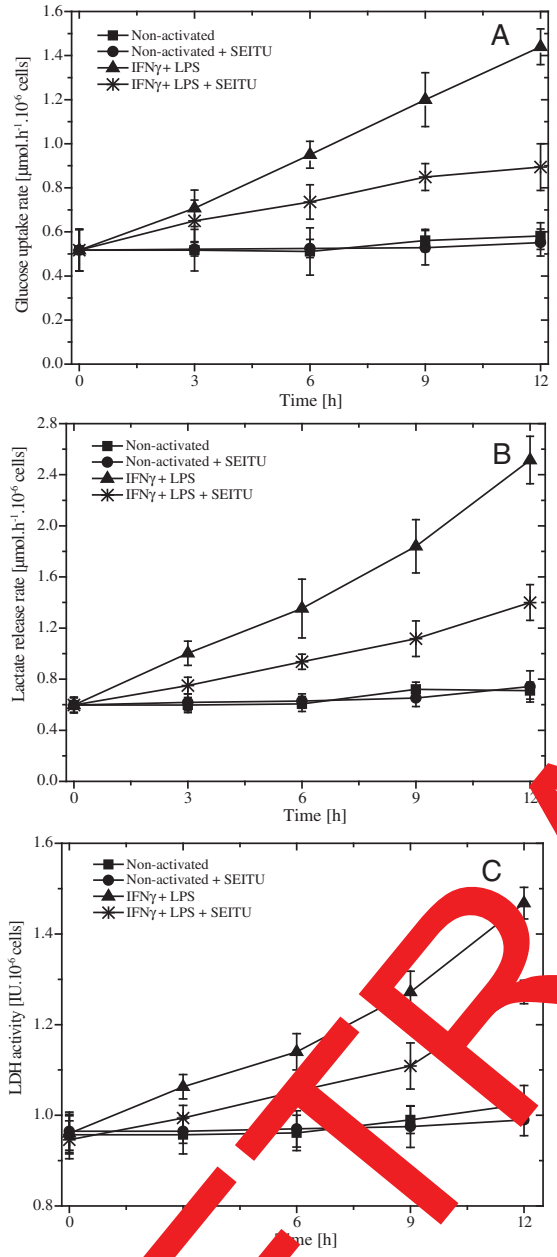

Fig. 2. Effect of activ[illegible] of MΦ [illegible] their glycol[illegible]tic metabolism. The rate of glucose uptake (A), rate [illegible] release (B) [illegible] LDH activity in cell homogenates (C) were deter[illegible]d in untrea[illegible] cells or in those activated with IFNγ and LP[illegible]ministrati[illegible]SEIT[illegible] partly prevented the increase in all three p[illegible]meters o[illegible]lycolytic m[illegible]sm that was observed in activated cells. M[illegible]±s.d., *n*=3[illegible] There were significant differences ($P<0.05$, one way ANO[illegible], Tukey's p[illegible]) in the glucose uptake rates, lactate release rates a[illegible]DH ac[illegible]ues betwee[illegible]e IFNγ + LPS + SEITU-treated group and all the oth[illegible]s at each sampling time, except at time zero.

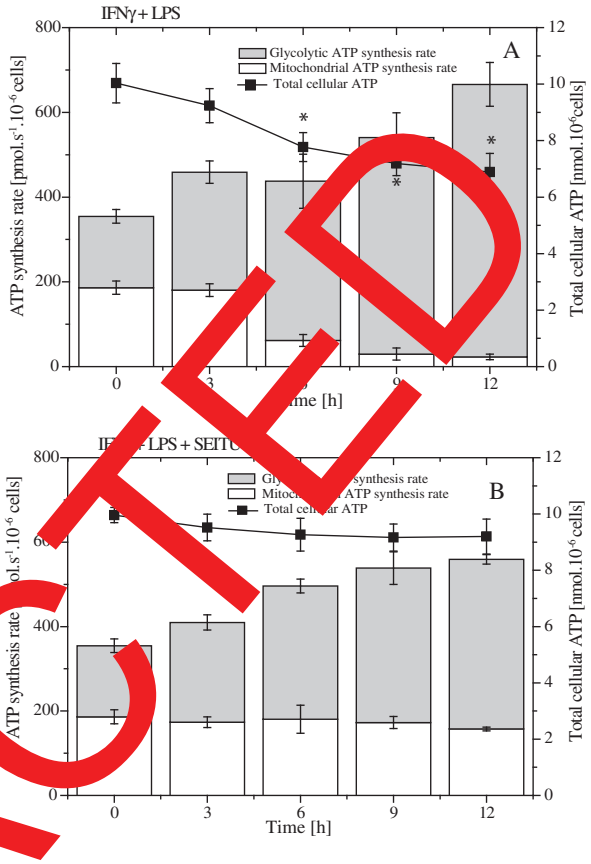

Fig. 3. Contribution of oxidative phosphorylation and glycolysis to ATP production in activated MΦ. Total cellular [ATP] and ATP synthesis rates (glycolytic and mitochondrial) of MΦ treated with IFNγ + LPS (A) and IFNγ + LPS + SEITU (B) are shown. Treatment with SEITU prevented the drop in mitochondrial synthesis of ATP and reduced the enhanced glycolytic production of ATP in activated MΦ. It also prevented the drop in total cellular [ATP]. Cellular [ATP] was determined by the luciferase assay, the rate of synthesis of ATP by glycolysis was computed from the lactate production rate, and the rate of synthesis of ATP by mitochondria was computed from the oligomycin-sensitive mitochondrial oxygen consumption rate, assuming a P:O ratio of 1:2.4. *, Total cellular ATP significantly different from values in non-activated cells (0 hour). Results are mean±s.d., *n*=5.

12 hours of activation, by 53% (Fig. 2C). Co-administration of SEITU at the time of activation partially suppressed the increase in each of these parameters of glycolytic metabolism (Fig. 2A-C).

Effect of MΦ activation on the generation and use of ATP

In non-activated MΦ oxidative phosphorylation and glycolysis contributed 186±17 and 168±16 pmol ATP second^{-1} 10^{-6} cells to the total cellular ATP synthesis, respectively. This maintained a steady-state cellular [ATP] of 10.3±0.5 nmol 10^{-6}cells (Fig. 3A,B). The rates of ATP synthesis by oxidative phosphorylation and glycolysis in these non-activated MΦ did not change significantly with time, and the steady state [ATP] was maintained at 9.8±0.35 nmol 10^{-6} cells after 12 hours (not shown). Following activation, the rate of ATP synthesis by oxidative phosphorylation declined to negligible values within 9 hours. By contrast, the rate of synthesis of glycolytic ATP increased to 643±52 pmol second^{-1} 10^{-6} cells at 12 hours. Despite the observed increase in total cellular ATP synthesis, however, the steady-state cellular [ATP] declined with incubation time, decreasing from 10.3±0.5 to 6.9±0.3 nmol ATP 10^{-6} cells after 12 hours (Fig. 3A). Co-administration of SEITU at the time of activation prevented the decrease in the synthesis of ATP by the mitochondria, partially reduced the increase in glycolysis and maintained the steady-state cellular [ATP] at ~93% of that of non-activated MΦ (Fig. 3B) ($P>0.05$, paired *t*-test).

Effect of MΦ activation on proliferation

Activation resulted in the complete arrest of MΦ proliferation, as shown by the lack of cell growth (density) and of incorporation of BrdU into the DNA of dividing cells (Fig. 4A,B). There was also a decline in cell viability to 73% after 24 hours (determined by Trypan Blue exclusion, data not shown). Co-administration of SEITU at the time of activation partially restored cell proliferation (Fig. 4A,B) and prevented the decline in viability (96% after 24 hours, data not shown). SEITU alone had no effect on the proliferation of non-activated cells.

Effect of MΦ activation on HIF1α stabilization

Activation of MΦ led to the accumulation of HIF1α protein, which was significant 1.5 hours after treatment (Fig. 5A,B). By 3 hours, the concentration of HIF1α had declined to that of the control but after 6 hours it began to increase again and at 12 hours was higher than it had been at 1.5 hours. Treatment with SEITU had no effect on the increase in HIF1α at 1.5 hours but it prevented the later increase (Fig. 5A,B). Silencing HIF1α prevented the activation-induced increase in HIF1α protein (shown at 12 hours in Fig. 5C), as did treatment with SEITU. Although the amount of iNOS protein did not change in HIF1α-silenced MΦ (Fig. 5C), there was a significant decrease in the generation of NO (Fig. 5D), further indicating the interaction of the two pathways.

Effect of silencing HIF1α on mitochondrial respiration and glycolysis in activated MΦ

Silencing HIF1α per se had no effect on any of the parameters of cell respiration. Furthermore, the responses to activation of control transfected (with scrambled siRNA) MΦ were similar to those of non-transfected activated MΦ (compare Fig. 5E with Fig. 1A, Fig. 2A). In activated HIF1α-silenced MΦ, sufficient NO was produced to abolish completely the spare respiratory capacity; however, the basal and oligomycin-sensitive mitochondrial O_2 uptake fell only by ~50% (Fig. 5E).

Activation of HIF1α-silenced MΦ resulted in a reduced upregulation of glycolysis, as shown by the reduction of lactate measured after 12 hours (Fig. 5F). Moreover, the combination of silencing HIF1α and treatment with SEITU completely abolished the upregulation of glycolysis. Silencing HIF1α also significantly downregulated the glycolytic metabolism of non-activated MΦ (Fig. 5F). The glycolytic rates of untransfected controls and control transfected MΦ were comparable, showing that transfection alone had no effect on the cells (not shown).

Effect of silencing HIF1α on the cellular ATP content

In non-activated MΦ, silencing HIF1α reduced the steady-state cellular ATP content by 30% (Fig. 5G). This reduction in ATP content was due to the diminished glycolytic ATP supply. The reduction in the ATP content was compounded by a reduction in the proliferation rate. The number of HIF1α-silenced MΦ increased by only 35% after 12 hours compared with an 80% increase in control transfected MΦ (data not shown). Activation of HIF1α-silenced MΦ for 12 hours reduced the cellular ATP content by a further 50%. This reduction in cellular ATP in response to activation could be totally reversed by inhibiting iNOS activity with SEITU (Fig. 5G).

Discussion

We have previously shown that, whereas neurons die rapidly after inhibition of mitochondrial respiration by NO, astrocytes develop a strong defence response that makes them resistant to pro-apoptotic

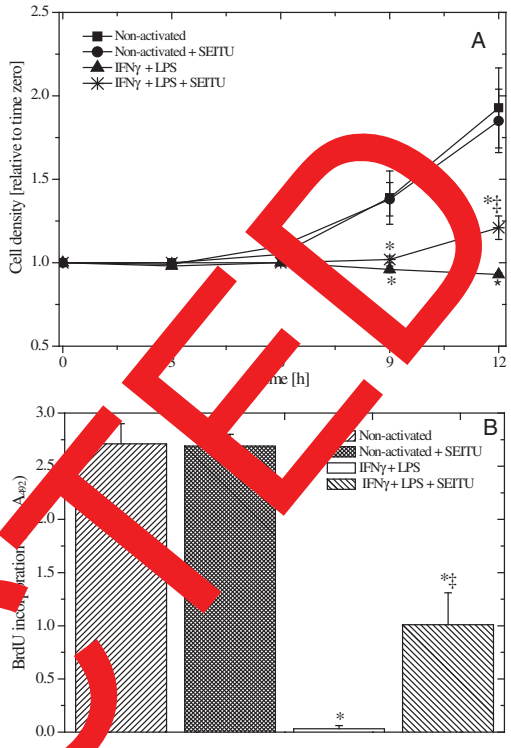

Fig. 4. Effect of activation of MΦ on their proliferation. Changes in cell density relative to the initial density are shown in A, and BrdU incorporation after 12 hours activation and 4 hours incubation with BrdU are shown in B. Activation led to complete arrest of cell proliferation that could be partially reversed by treatment with SEITU. *, Significantly different from values in non-activated cells; ‡, Significantly different from IFNγ + LPS-treated cells ($P<0.05$, ANOVA, Tukey's test). Results are mean±s.d., $n=5$.

agents (Almeida et al., 2001). A significant metabolic difference between these two cell types is that, following inhibition of mitochondrial respiration, the latter are able to activate glycolysis, which probably maintains their mitochondrial membrane potential for a considerable period (Beltran et al., 2000b). Thus, activation of glycolysis, which has long been known to occur during inflammatory activation of cells and tissues, is a key component of the response of some cells to injury and may explain, at least in part, their differential sensitivity to damage. In spite of this, not much is known about the metabolic adaptation and the signalling mechanisms of different cells in response to injury.

In this study, we have used the murine macrophage cell line J774.A1 to investigate the generation and use of ATP after activation by IFNγ and LPS. Furthermore, we have studied the involvement of NO and HIF1α in this process. Under basal conditions, non-activated MΦ respired using 48% of the total mitochondrial respiratory capacity. Approximately 80% of the O_2 consumed by the mitochondria was used by the electron transport chain to respire and generate 53% of the total cellular ATP; the rest of the ATP was generated by glycolysis. The remaining 20% of the O_2 consumed by the mitochondria was used by the proton leak across the inner mitochondrial membrane. With the induction of iNOS and subsequent production of NO, mitochondrial O_2 consumption declined progressively following activation. This decline became significant at 4 hours and mitochondrial O_2 consumption reached 27% of the control value after 12 hours of

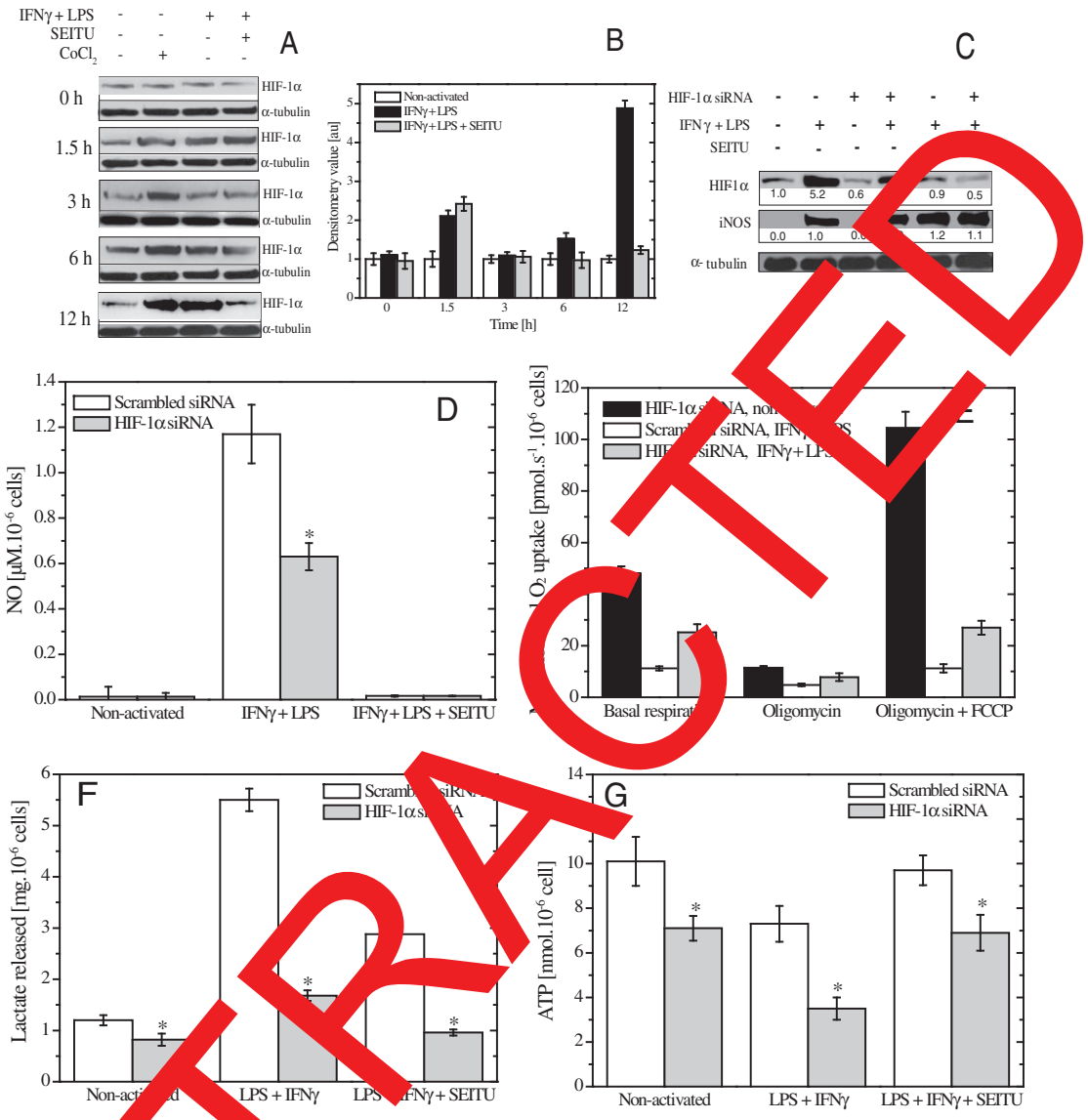

Fig. 5. Effect of activation of MΦ on the stabilization of HIF1α. (A) The time course of HIF1α stabilization following activation and (B) the corresponding densitometry values normalized with α-tubulin and relative to non-activated controls. Cobalt chloride ($CoCl_2$) was used as a positive control for HIF1α in A. (C) Cells were transfected with HIF1α siRNA or scrambled siRNA as a control. After 24 hours they were treated with the agents indicated and incubated for 12 hours. Treatment with IFNγ + LPS resulted in stabilization of HIF1α under normoxic conditions. This was reduced in the cells in which HIF1α had been silenced, and in those treated with SEITU. Densitometry values, normalized with α-tubulin and relative to that of control transfected MΦ (in the case of HIF1α) and control transfected and activated MΦ (in the case of iNOS) are shown below each lane. (D) Silencing HIF1α reduced the generation of NO and (E) partially preserved mitochondrial oxygen consumption in activated MΦ. (F) The upregulation of glycolysis in activated MΦ was attenuated by silencing HIF1α and by treatment with SEITU; it was completely abolished by a combination of the two treatments. (G) The cellular ATP content was reduced in MΦ in which HIF1α had been silenced and was reduced by activation, an effect that was prevented by SEITU. *, Significantly different from control transfected values. Results are mean±s.d., n=3-5, and representative western blots are shown.

activation. The majority of this decrease was due to the decline in oxidative phosphorylation as the proton leak-related O_2 consumption, which is mainly determined by the mitochondrial membrane potential (Yadava and Nicholls, 2007; Parker et al., 2008), was reduced by only ~20%. This suggests that the mitochondrial membrane potential was at least partially maintained during that period, most probably by using glycolytically generated ATP (Beltran et al., 2000b). The spare respiratory capacity was significantly reduced at 3 hours after activation. The fact that this could be prevented by SEITU, even though there was no detectable extracellular release of NO at this time, indicates that it was attributable to NO.

Interestingly, as mitochondrial O_2 consumption decreased, there was an increase in the non-mitochondrial O_2 consumption. This constituted ~50% of the total cellular O_2 consumption at 12 hours and ~100% at 24 hours after MΦ activation. The non-mitochondrial O_2 consumption was partially blocked by HbO_2 and completely abolished by treatment with SEITU, indicating that it is due to the activity of iNOS, which is an O_2-dependent enzyme (Stuehr and Nathan, 1989; Leone et al., 1991). The proportion of non-

mitochondrial O_2 consumption used by iNOS and that used for the oxidation of NO remains to be investigated.

Within 12 hours of MΦ activation, ATP synthesis by the mitochondria declined to negligible values, whereas that provided by glycolysis increased by ~400%, thus doubling the total cellular ATP supply. Despite the increase in total cellular ATP synthesis, the steady-state [ATP] decreased, indicating that the cellular ATP demand might be greater than the supply. Treatment of cells with SEITU at the time of activation maintained the steady-state cellular [ATP] at a level similar to controls by maintaining the generation of ATP by the mitochondria together with a smaller increase in glycolysis. This small increase in glycolysis is most probably attributable to the upregulation of glucose transporters and glycolytic enzymes by HIF1, owing to stabilization of its α-subunit during the early hours of activation, which was not affected by inhibiting NO synthesis. Thus, it appears that glycolysis can be upregulated to the point at which it more than compensates for the loss of ATP generated by oxidative phosphorylation. This increase, however, is not sufficient to compensate for the increased requirement for ATP during activation, so that inhibition of proliferation and cell death ensue.

One of the main contributors to the upregulation of glycolysis is the stabilization of HIF1α. HIF1α, which is stabilized in hypoxia due to inhibition of the O2-sensitive enzymes involved in its degradation (Semenza, 2007), can also be stabilized by a variety of other mechanisms, including the action of NO adducts (Mateo et al., 2003; Kasuno et al., 2004; Peyssonnaux et al., 2005; Quintero et al., 2006) and reactive oxygen species (ROS) (for a review, see Chandel et al., 2000). In our experiments, we found that HIF1α was stabilized after MΦ activation in a biphasic manner. The early stabilization observed after 1.5 hours was insensitive to the treatment with SEITU. We are currently investigating the mechanism of this early stabilization. Our accumulating evidence, and previously published observations (Quintero et al., 2006), suggest that it is also dependent on ROS. The later stabilization, however, was dependent on the generation of NO as it could be abolished by treatment with SEITU. Inhibition of NO synthesis was accompanied by restoration of mitochondrial O_2 consumption, disappearance of the non-mitochondrial consumption and a significant reduction in the upregulation of glycolysis. Furthermore, we observed that silencing HIF1α reduced the production of NO to ~50% of that of control transfected cells, even though the amount of iNOS protein remained unchanged. It has previously been reported that HIF1α upregulates transcriptional activation and accumulation of iNOS protein (Jung et al., 2000). Under our experimental conditions, however, iNOS was induced by the inflammatory agents IFNγ+LPS, and HIF1α appears to upregulate iNOS activity rather than the amount of the enzyme. The effect of activation of MΦ on glycolysis depends on both iNOS activity and stabilization of HIF1α, as they appear to operate in a positive-feedback loop, enhancing each other's production. Indeed, combination of silencing HIF1α and inhibiting iNOS activity completely abolished the upregulation of glycolysis. It has recently been reported that HIF1α stabilization during hypoxia results in a reduction in oxidative phosphorylation by increasing the expression of PDK1 (Papandreou et al., 2006; Kim et al., 2006), the enzyme responsible for the conversion of pyruvate into acetyl coenzyme A. In our experiments, however, the main metabolic defect was dependent on the generation of NO and was completely reversed following its inhibition with SEITU. How NO-dependent inhibition of mitochondria and upregulation of PDK 1 may be interacting to increase glycolysis remains to be investigated, not only in inflammation but in other conditions.

In summary, activation of MΦ with IFNγ and LPS leads to a mitochondrial defect and to the stabilization of HIF1α; in both of these processes NO plays a prominent role. The consequent switch towards glycolytic metabolism, although capable of increasing dramatically the supply of ATP, is insufficient to provide for the requirements of the activated cells, leading to a decrease in proliferation and to cell death. It is likely that such a mechanism not only underlies the pathophysiology of septic shock but might also be a significant component of acute and chronic inflammatory conditions and also of some degenerative processes.

Materials and Methods

Reagents

Dulbecco's Modified Eagle medium (DMEM), penicillin, streptomycin and glutamine were from Invitrogen. LPS of bacterial strain *Staphylococcus typhosa* 0901 was from Difco, and murine IFNγ was from Insight Biotech. The lactate assay kit was from Trinity Biotech, the luciferase and ATP assay kit ATPlite was from Perkin Elmer and the 5-bromo-2-deoxyuridine (BrdU) proliferation ELISA (colorimetric) kit was from Roche. All other reagents were from Sigma-Aldrich.

Cell culture, inflammatory activation and preparation of MΦ

The murine MΦ cell line J774A.1 (ATCC TIB 67) was maintained in suspension in stirred bottles (Techne) in DMEM containing 25 mM D-glucose, 10% FCS, 2 mM L-glutamine, 100 units ml^{-1} penicillin and 100 μg ml^{-1} streptomycin. Activation was carried out by resuspending cells in a stirrer bottle at a density of 0.4-0.5×10^6 cells ml^{-1} in fresh medium supplemented with 10 U ml^{-1} murine IFNγ plus 10 ng ml^{-1} LPS. In one group the activity of iNOS was inhibited by co-administration of 500 μM S-ethyl isothiourea (SEITU) at the same time as IFNγ and LPS, in order to distinguish the NO-dependent and -independent components of inflammation. For experiments that involved ATP determinations, DMEM without Phenol Red was used. At different time points after activation, a 15 ml aliquot was removed and subdivided for protein, enzyme activity and ATP assays (1 ml for each assay), and the remaining 12 ml was used for respirometry. The samples for enzyme assays were centrifuged, washed once and resuspended in PBS, snap-frozen in liquid nitrogen and stored at –80°C until analysis. On the day of the assay, the samples were thawed and Triton X-100 was added to 0.25% final concentration for complete cell homogenization. The samples for ATP assay were lysed with mammalian cell lysis solution (provided with the kit) and stored at –80°C until analysis. The 12 ml sample for respirometry was centrifuged and the supernatant was frozen at –20°C until needed for glucose, lactate and NO_2^- determination. The pellet was resuspended in fresh medium at a cell density of 2×10^6 cells ml^{-1}. After adding a 1.2 ml cell suspension to the respirometry chamber and stirring, a 50 μl suspension was removed for cell counting with Trypan Blue staining. The chambers were closed and respirometric experiments were carried out, with titration protocols as described in the next section.

Respirometry and NO measurements

Cellular O_2 consumption and NO production were measured simultaneously in an air-tight twin glass chamber respirometer (Rank Brothers, Cambridge, UK) maintained at 37°C. Each chamber contained a Clark-type polarographic O_2 electrode and an NO nanosensor (amiNO-600, Innovative Instruments, FL). The cell suspension was stirred with glass-coated stirrer bars at 750 rpm. The signals from the O_2 and NO sensors were input into a four-channel potentiostat and analogue-to-digital converter (ESA Biosciences), and sampled at 1 Hz by online data acquisition software (Biostat-ESA Biosciences).

The NO nanosensors were calibrated daily as previously described (Tsukahara et al., 1994). The average sensitivity of the NO sensors was ~250 pA nM^{-1} NO. The O_2 electrodes were calibrated daily using a two-point calibration procedure as previously described (Hollis et al., 2003). The cellular O_2 consumption was determined by subtracting the instrumental background O_2 flux from the apparent O_2 flux, as previously described (Hollis et al., 2003).

Intact cell respirometry protocol

We designed an intact cell respirometry protocol that enables us to analyze the different states of mitochondrial respiration in situ in cell growth medium. Basal cellular O_2 consumption was recorded without metabolic inhibitors or uncouplers. The ATP synthase was then inhibited with 2 μg.ml^{-1} oligomycin, followed by uncoupling of the respiratory chain from oxidative phosphorylation by a stepwise titration of carbonyl cyanide *p*-(trifluoromethoxy) phenylhydrazone (FCCP) to achieve maximal O_2 consumption. Mitochondrial O_2 consumption was then completely inhibited by sequential addition of 0.5 μM myxothiazol (to inhibit complex III) and 500 μM KCN (to inhibit CcO). Finally, the activity of iNOS, and thus the O_2 consumption by this enzyme, was inhibited by 500 μM SEITU. In experiments that involved quenching NO with HbO_2, 10 μM of this compound was added before SEITU.

The different components of cellular/mitochondrial O_2 consumption were distinguished as follows:

Mitochondrial O_2 consumption = (basal consumption by the cell) – (myxothiazol and cyanide-insensitive consumption);

O_2 consumption due to oxidative phosphorylation = (basal consumption) – (oligomycin-insensitive consumption);

Spare respiratory capacity = (FCCP-uncoupled maximal O_2 consumption) – (basal consumption);

Non-mitochondrial O_2 consumption = myxothiazol and cyanide-insensitive O_2 consumption.

Cell proliferation assay

In addition to microscopic counting, cell proliferation was assessed by incorporation of the thymidine analogue 5-bromo-2′-deoxyuridine (BrdU) into the DNA of proliferating cells, using the cell proliferation ELISA BrdU colorimetric kit. Cells were grown overnight and resuspended in fresh medium containing the following treatments: IFNγ plus LPS, or IFNγ plus LPS and SEITU, or SEITU alone, or no treatment, and incubated for 12 hours. The cell density of each treatment was adjusted to 0.5×10^6 cells ml^{-1} and a 100 μl sample (replicate of 5) was placed in a 96-well plate. BrdU was added to a final concentration of 10 μM and the samples were processed further according to manufacturer's recommendation.

Biochemical assays

All spectrophotometric assays were performed in 96-well plates in 5-7 replicates and the optical density readings were carried out with the SpectraMax-Plus plate reader by acquiring data using the SoftMaxPro software (Molecular Devices).

Glucose concentration was determined using a glucose oxidase-based assay with a slight modification of the protocol of a commercially available kit. In brief, the samples were diluted 1:100 with distilled water and a 50 μl sample was mixed with 50 μl glucose oxidase reagent and processed further, according to the manufacturer's recommendation.

Lactate concentration was determined using a lactate oxidase-based assay. A 5 μl aliquot was added to a 96-well plate followed by 100 μl lactate reagent and processed further according to the manufacturer's recommendation.

As the cell density of the controls and IFNγ plus LPS and SEITU-treated cells was increasing during the course of incubation, glucose consumption and lactate release rates were computed by correcting for the time derivative of the changing cell density.

Lactate dehydrogenase (LDH) assay was performed using a slight modification of the method of (Bergmeyer and Bernt, 1974). Briefly, 90 μl of cell homogenate was added into 96-well plate followed by 160 μl reaction mixture [15.6 mM pyruvate and 0.47 mM NADH in Tris-HCl buffer (pH 7.1)]. The reaction mixture was shaken in the spectrophotometer and enzyme activity was recorded by measuring the rate of disappearance of NADH (ΔA_{340}) for 10 minutes in kinetic mode. The linear component of the absorbance kinetics was used in the computation of enzyme activity, which was normalized with cell number. Total cell protein concentration in the supernatant was determined using the Bicinchoninic acid (BCA) Protein Assay Reagent (Thermo Scientific), with bovine serum albumin (BSA) as standard.

Cellular ATP content was determined using a luciferase-based assay kit ATPlite, according to the recommended procedure. Briefly, 100 μl of cell homogenate was added to a 96-well plate followed by 50 μl substrate buffer. Luminescence was counted using a Microplate Scintillation and Luminescence Counter (Packard BioSciences) after mixing and 10 minutes dark adaptation of the plate. ATP standards and blanks were incorporated in each reading.

Glycolytic ATP synthesis rate was computed from lactate release rate with the assumption of a lactate:ATP ratio of 1. The rate of ATP synthesis by oxidative phosphorylation was computed from the oligomycin-sensitive mitochondrial O_2 consumption by assuming stoichiometric moles of ATP synthesis:moles of O_2 consumed (P:O ratio) to be 1:2.4 (Brand, 2005).

Gene silencing with small interfering RNA (siRNA)

Commercially available ON-TARGETplus SMARTpool siRNA against the mouse HIF1α subunit and a non-targeting AllStars Negative Control siRNA conjugated to Alexa Fluor 555 were purchased from Dharmacon RNA Technologies and Qiagen, respectively. Transfection of J774.A1 MΦ with the siRNAs to generate HIF1α knockdown cells was performed using Lipofectamine RNAiMAX Transfection Reagent (Invitrogen) according to the manufacturer's instructions using a reverse transfection protocol. Cells for ATP determination were transfected in 96-well black plates in Phenol Red-free medium.

After 24 hours of transfection, cells were treated with IFNγ + LPS ± SEITU and incubated for a further 12 hours. The conditioned medium was removed and stored at –20°C for glucose, lactate and NO_2^- assays. Cells were then used for ATP determination, respirometry or western blotting. Cell viability was determined by Trypan Blue staining.

Protein electrophoresis and western blotting

Protein for the time course of HIF1α stabilization was obtained from cells grown in a stirrer bottle, as explained under 'Cell culture, inflammatory activation and preparation of MΦ'. Positive HIF1α controls were obtained by treating cells with 100 μM $CoCl_2$, which activates HIF1α in an O_2-independent manner. Whole-cell homogenates were prepared by scraping off and/or resuspending cells in ice-cold CytoBuster Protein Extraction Reagent (Novagen) containing Complete Protease Inhibitor Cocktail Tablet (Roche) and incubating on ice for 10 minutes. Samples were centrifuged at 13,000 ***g*** (4°C) to pellet cell debris. Protein concentration in the supernatant was determined using the Bicinchoninic acid (BCA) Protein Assay Reagent. Sample aliquots were mixed with Laemmli buffer, boiled for 10 minutes and 25 μg total protein was fractionated using pre-cast 4-15% gradient SDS-PAGE gel electrophoresis (BioRad). Proteins were transferred to Hybond-ECL nitrocellulose membranes (GE Healthcare) and subjected to immunoblot assay using rabbit polyclonal antibodies against iNOS (BD Biosciences), mouse monoclonal antibodies against HIF1α and α-tubulin (Abcam) and horseradish peroxidase conjugated goat antibody against mouse IgG (Dako) at 1:2,000 dilution. The chemiluminescence signal was developed using ECL Plus Western Blotting Detection Reagents (GE Healthcare).

Statistical analysis

Values are presented as mean±s.e.m. n=3-7 repeats and each repeat was replicated at least three times. Comparison between two groups was carried out using a paired sample *t*-test, and between three or more groups using one way ANOVA and the Tukey's or Dunnett's post hoc test, as appropriate.

We are grateful to Cecilia Andreassi and Annie Higgs for reading the manuscript and for their very useful comments and suggestions. We also thank Leanne Boorn for valuable assistance in some of the experiments.

References

Almeida, A., Almeida, J., Bolanos, J. P. and Moncada, S. (2001). Different responses of astrocytes and neurons to nitric oxide: the role of glycolytically generated ATP in astrocyte protection. *Proc. Natl. Acad. Sci. USA* **98**, 15294-15299.

Beltran, B., Orsi, A., Clementi, E. and Moncada, S. (2000a). Oxidative stress and S-nitrosylation of proteins in cells. *Br. J. Pharmacol.* **129**, 953-960.

Beltran, B., Mathur, A., Duchen, M. R., Erusalimsky, J. D. and Moncada, S. (2000b). The effect of nitric oxide on cell respiration: a key to understanding its role in cell survival or death. *Proc. Natl. Acad. Sci. USA* **97**, 14602-14607.

Bergmeyer, H. U. and Bernt, E. (1974). *Enzymatic Assay of L-Lactic dehydrogenase*. New York: Academic Press.

Boushel, R., Gnaiger, E., Schjerling, P., Skovbro, M., Kraunsoe, R. and Dela, F. (2007). Patients with type 2 diabetes have normal mitochondrial function in skeletal muscle. *Diabetologia* **50**, 790-796.

Brand, M. D. (2005). The efficiency and plasticity of mitochondrial energy transduction. *Biochem. Soc. Trans.* **33**, 897-904.

Brand, M. D., Pakay, J. L., Ocloo, A., Kokoszka, J., Wallace, D. C., Brookes, P. S. and Cornwall, E. J. (2005). The basal proton conductance of mitochondria depends on adenine nucleotide translocase content. *Biochem. J.* **392**, 353-362.

Brealey, D., Brand, M., Hargreaves, I., Heales, S., Land, J., Smolenski, R., Davies, N. A., Cooper, C. E. and Singer, M. (2002). Association between mitochondrial dysfunction and severity and outcome of septic shock. *Lancet* **360**, 219-223.

Brown, G. C. and Cooper, C. E. (1994). Nanomolar concentrations of nitric oxide reversibly inhibit synaptosomal respiration by competing with oxygen at cytochrome oxidase. *FEBS Lett.* **356**, 295-298.

Chandel, N. S., McClintock, D. S., Feliciano, C. E., Wood, T. M., Melendez, J. A., Rodriguez, A. M. and Schumacker, P. T. (2000). Reactive oxygen species generated at mitochondrial complex III stabilize hypoxia-inducible factor-1alpha during hypoxia. A mechanism of O_2 sensing. *J. Biol. Chem.* **275**, 25130-25138.

Cleeter, M. W. J., Cooper, J. M., Darley-Usmar, V. M., Moncada, S. and Schapira, A. H. V. (1994). Reversible inhibition of cytochrome c oxidase, the terminal enzyme of the mitochondrial respiratory chain, by nitric oxide. *FEBS Lett.* **345**, 50-54.

Clementi, E., Brown, G. C., Feelisch, M. and Moncada, S. (1998). Persistent inhibition of cell respiration by nitric oxide: crucial role of S-nitrosylation of mitochondrial complex I and protective action of glutathione. *Proc. Natl. Acad. Sci. USA* **95**, 7631-7636.

Cramer, T., Yamanishi, Y., Clausen, B. E., Forster, I., Pawlinski, R., Mackman, N., Haase, V. H., Jaenisch, R., Corr, M., Nizet, V. et al. (2003). HIF-1alpha is essential for myeloid cell-mediated inflammation. *Cell* **112**, 645-657.

Ebert, B. L., Firth, J. D. and Ratcliffe, P. J. (1995). Hypoxia and mitochondrial inhibitors regulate expression of glucose transporter-1 via distinct Cis-acting sequences. *J. Biol. Chem.* **270**, 29083-29089.

Escames, G., Lopez, L. C., Ortiz, F., Lopez, A., Garcia, J. A., Ros, E. and Acuna-Castroviejo, D. (2007). Attenuation of cardiac mitochondrial dysfunction by melatonin in septic mice. *FEBS J.* **274**, 2135-2147.

Frost, M. T., Wang, Q., Moncada, S. and Singer, M. (2005). Hypoxia accelerates nitric oxide-dependent inhibition of mitochondrial complex I in activated macrophages. *Am. J. Physiol. Regul. Integr. Comp. Physiol.* **288**, R394-R400.

Hollis, V. S., Palacios-Callender, M., Springett, R. J., Delpy, D. T. and Moncada, S. (2003). Monitoring cytochrome redox changes in the mitochondria of intact cells using multi-wavelength visible light spectroscopy. *Biochim. Biophys. Acta* **1607**, 191-202.

Jiang, B. H., Semenza, G. L., Bauer, C. and Marti, H. H. (1996). Hypoxia-inducible factor 1 levels vary exponentially over a physiologically relevant range of O_2 tension. *Am. J. Physiol., Cell Physiol.* **271**, C1172-C1180.

Jung, F., Palmer, L. A., Zhou, N. and Johns, R. A. (2000). Hypoxic regulation of inducible nitric oxide synthase via hypoxia inducible factor-1 in cardiac myocytes. *Circ. Res.* **86**, 319-325.

Kasuno, K., Takabuchi, S., Fukuda, K., Kizaka-Kondoh, S., Yodoi, J., Adachi, T., Semenza, G. L. and Hirota, K. (2004). Nitric oxide induces hypoxia-inducible factor 1 activation that is dependent on MAPK and phosphatidylinositol 3-kinase signaling. *J. Biol. Chem.* **279**, 2550-2558.

Kim, J. W., Tchernyshyov, I., Semenza, G. L. and Dang, C. V. (2006). HIF-1-mediated expression of pyruvate dehydrogenase kinase: A metabolic switch required for cellular adaptation to hypoxia. *Cell Metab.* **3**, 177-185.

Leone, A. M., Palmer, R. M., Knowles, R. G., Francis, P. L., Ashton, D. S. and Moncada, S. (1991). Constitutive and inducible nitric oxide synthases incorporate molecular oxygen into both nitric oxide and citrulline. *J. Biol. Chem.* **266**, 23790-23795.

Lin, M. T. and Beal, M. F. (2006). Mitochondrial dysfunction and oxidative stress in neurodegenerative diseases. *Nature* **443**, 787-795.

Mateo, J., Garcia-Lecea, M., Cadenas, S., Hernandez, C. and Moncada, S. (2003). Regulation of hypoxia-inducible factor-1alpha by nitric oxide through mitochondria-dependent and -independent pathways. *Biochem. J.* **376**, 537-544.

Mogensen, M., Sahlin, K., Fernstrom, M., Glintborg, D., Vind, B. F., Beck-Nielsen, H. and Hojlund, K. (2007). Mitochondrial respiration is decreased in skeletal muscle of patients with type 2 diabetes. *Diabetes* **56**, 1592-1599.

Moncada, S. and Erusalimsky, J. D. (2002). Does nitric oxide modulate mitochondrial energy generation and apoptosis? *Nat. Rev. Mol. Cell. Biol.* **3**, 214-220.

Nicolson, G. L. (2007). Metabolic syndrome and mitochondrial function: molecular replacement and antioxidant supplements to prevent membrane peroxidation and restore mitochondrial function. *J. Cell Biochem.* **100**, 1352-1369.

Orsi, A., Beltran, B., Clementi, E., Hallen, K., Feelisch, M. and Moncada, S. (2000a). Continuous exposure to high concentrations of nitric oxide leads to persistent inhibition of oxygen consumption by J774 cells as well as extraction of oxygen by the extracellular medium. *Biochem. J.* **346**, 407-412.

Orsi, A., Rees, D. D., Beltran, B. and Moncada, S. (2000b). Physiological regulation and pathological inhibition of tissue respiration by nitric oxide in vivo. In *The Biology of Nitric Oxide, Part 7* (ed. S. Moncada, L. E. Gustafsson, N. P. Wiklund and E. A. Higgs). London: Portland Press.

Papandreou, I., Cairns, R. A., Fontana, L., Lim, A. L. and Denko, N. C. (2006). HIF-1 mediates adaptation to hypoxia by actively downregulating mitochondrial oxygen consumption. *Cell Metab.* **3**, 187-197.

Parker, N., Affourtit, C., Vidal-Puig, A. J. and Brand, M. D. (2008). Energisation-dependent endogenous activation of proton conductance in skeletal muscle mitochondria. *Biochem. J.* **412**, 131-139.

Peyssonnaux, C., Datta, V., Cramer, T., Doedens, A., Theodorakis, E. A., Gallo, R. L., Hurtado-Ziola, N., Nizet, V. and Johnson, R. S. (2005). HIF-1alpha expression regulates the bactericidal capacity of phagocytes. *J. Clin. Invest.* **115**, 1806-1815.

Protti, A., Carre, J., Frost, M. T., Taylor, V., Stidwill, R., Rudiger, A. and Singer, M. (2007). Succinate recovers mitochondrial oxygen consumption in septic rat skeletal muscle. *Crit. Care Med.* **35**, 2150-2155.

Quintero, M., Brennan, P. A., Thomas, G. J. and Moncada, S. (2006). Nitric oxide is a factor in the stabilization of hypoxia-inducible factor-1{alpha} in cancer: Role of free radical formation. *Cancer Res.* **66**, 770-774.

Rees, D. D., Monkhouse, J. E., Cambridge, D. and Moncada, S. (1998). Nitric oxide and the haemodynamic profile of endotoxin shock in the conscious mouse. *Br. J. Pharmacol.* **124**, 540-546.

Schapira, A. H. (2006). Mitochondrial disease. *Lancet* **368**, 70-82.

Schweizer, M. and Richter, C. (1994). Nitric oxide potently and reversibly deenergizes mitochondria at low oxygen tension. *Biochem. Biophys. Res. Commun.* **204**, 169-175.

Semenza, G. L. (2007). Hypoxia-inducible factor 1 (HIF-1) pathway. *Sci. STKE* 2007, cm8.

Semenza, G. L., Roth, P. H., Fang, H. M. and Wang, G. L. (1994). Transcriptional regulation of genes encoding glycolytic enzymes by hypoxia-inducible factor 1. *J. Biol. Chem.* **269**, 23757-23763.

Stuehr, D. J. and Nathan, C. F. (1989). Nitric oxide: a macrophage product responsible for cytostasis and respiratory inhibition in tumor target cells. *J. Exp. Med.* **169**, 1543-1555.

Tsukahara, H., Gordienko, D. V., Tonshoff, B., Gelato, M. C. and Goligorsky, M. S. (1994). Direct demonstration of insulin-like growth factor-I-induced nitric oxide production by endothelial cells. *Kidney Int.* **45**, 598-604.

Whitton, P. S. (2007). Inflammation as a causative factor in the aetiology of Parkinson's disease. *Br. J. Pharmacol.* **150**, 963-976.

Yadava, N. and Nicholls, D. G. (2007). Spare respiratory capacity rather than oxidative stress regulates glutamate excitotoxicity after partial respiratory inhibition of mitochondrial complex I with rotenone. *J. Neurosci.* **27**, 7310-7317.